

MODELLING AND PERFORMANCE EVALUATION OF ANTI-LOCK BRAKING SYSTEM

DANKAN GOWDA V.^{1,*}, RAMACHANDRA A. C.²,
THIPPESWAMY M. N.³, PANDURANGAPPA C.⁴, RAMESH NAIDU P.⁵

^{1,2,3,5}Department of Computer Science and Engineering, Nitte Meenakshi Institute of
Technology, Bangalore, Karnataka 560064, India

⁴Department of Mathematics, UBDT College of Engineering,
Davangere, Karnataka 577004, India

*Corresponding Author: dankanies@gmail.com

Abstract

Current Antilock Braking System (ABS) is controlled based on wheel deceleration and slip. It is used in present automobiles for improved safety and consistency. It is basically an active protection system currently implemented in most of the automobiles and can avoid the wheels from locking during heavy braking. This paper investigates the effect of the proposed sliding mode controller (SMC) based Antilock Braking System including a longitudinal wheel dynamics simulation, a brake torque actuation, brake pressure modulation and angular wheel speed. Mathematical description of Lugre Friction model, Burckhardt Friction model is presented. An antilock braking system using a bang-bang control law to achieve the wheel slip within the specified range is discussed. The proposed controller performance evolution in terms of brake pressure modulation, vehicle velocity, wheel slip and stopping distance are compared with, in absence of wheel speed controller, bang-bang controller, ABS with Lugre Friction Model (LFM) and ABS with Burckhardt Friction Model (BFM).

Keywords: Active safety system, Antilock braking system, Burckhardt friction model, Lugre friction model, MATLAB-Simulink, Sliding mode controller, Wheel slip controller.

1. Introduction

Road safety research has increased exponentially since the 1950s [1]. In 1990, a little over 250 articles about road safety were published, whereas in 2010 there were 2,000 publications. There are various ways to improve road safety such as placing street lighting, improving road quality, and installing road signs. The car itself is another factor, which offers many ways to improve the safety of the driver or passengers. In general, it can be said that such safety systems are divided into active and passive systems. Passive safety systems reduce damage after an impact. Active safety systems are meant to prevent accidents and are, thus, active prior to the event of a potential crash.

Examples of passive safety systems are airbags, seat belts, and deformation zones. Hulten [2] explained that the development of passive safety is assumed to be near its limit. ABS is an example of an active safety system. The initial goal of ABS was to maintain steer-ability during heavy braking. To achieve this, it prevents wheels from locking. Steering then remains possible, and the brake distance is often shortened as well. Nowadays, the system is fundamental in other safety systems as well, such as Braking Assist System (BAS), Electronic Stability Control (ESC), Cornering Brake Control (CBC), and Traction Control (TC).

Currently, ABS is controlled based on wheel deceleration and slip. ABS performance of the current algorithm by Bosch already performs well. It is, however, an algorithm based on many heuristics, which makes it hard to tune. Considering there are still road surfaces and situations for which, ABS could be improved, researchers have been trying to find a more mathematical approach to the algorithm [3-8]. With the basis of the technology that is easier to interpret, it is expected that ABS could be more stable and robust on more slippery road surfaces. This mainly concerns wet, snowy, and icy roads. Another challenge in the development of ABS in the velocities at which, the algorithm works. At lower velocity, it becomes increasingly hard to control, as the wheels tend to lock more easily. In this paper, we mainly focused on modelling of ABS controller using various non-linear controllers and finally the performance in terms of vehicle stopping distance and stopping time of the proposed algorithm is compared with an existing technique [9, 10].

2. LuGre Friction Model

At the minute level, two surfaces reach different asperities. These asperities are spoken to with bristles, and the fibres divert like a spring when there is a relative speed between the two surfaces. According to Gowda and Chakrasali [11] and Akermann and Sienel [12], make use of first-order derivatives, the average deflection of bristles, Z is modelled. Friction Interface in the LuGre model is shown in Fig. 1.

$$\frac{dz}{dt} = v_r - \frac{|v_r|}{g(v_r)} z \quad (1)$$

where v_r indicates the two surfaces relative velocity. Deflection is indicated by the first term, which is proportional to the integral of the v_r deflection z indicated by the second term and is given by:

$$z_{ss} = \frac{v_r}{|v_r|} g(v_r) = g(v_r) \operatorname{sgn}(v_r) \quad (2)$$

Under the condition of steady-state, that is $\frac{dz}{dt} = 0$, (i.e., when $v = K$ (constant)).

The static coefficient of friction of LuGre model is achieved more than the dynamic coefficient of friction with the help of function $g(v)$. The possible form of $g(v)$ is given by

$$g(v) = \frac{1}{\sigma_0} \left[\mu_c + (\mu_s - \mu_c) \exp - \left(\frac{v_r}{v_s} \right)^2 \right] \tag{3}$$

The LuGre friction force due to the bending of Bristles is given by:

$$F_x = \left(\sigma_0 z + \sigma_1 \frac{dz}{dt} + \sigma_2 v_r \right) F_z \tag{4}$$

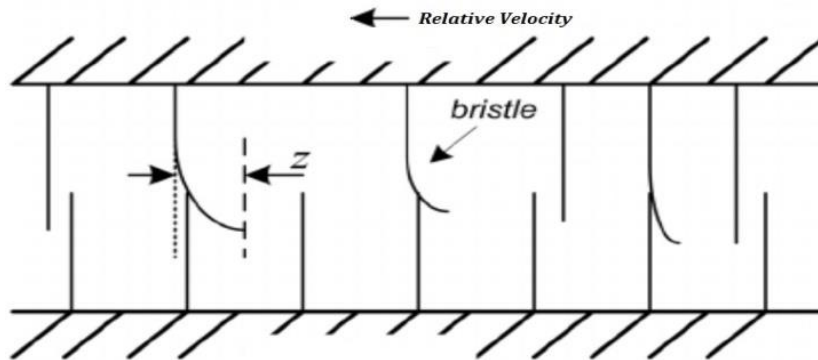


Fig. 1. Friction interface in LuGre model.

2.1. Vehicle dynamics

A streamlined quarter auto vehicle demonstrates experiencing impeccably straight-line braking move has been considered [13-15]. Assumptions that are considered for simulation are:

- No steering signal and vehicle is moving only along a straight-line path.
- Damping effect is zero and assumes that vertical forces are constant.

The equation of motion is given by:

$$\frac{dv}{dt} = - \frac{F_x}{m} \tag{5}$$

$$\frac{d\omega}{dt} = \frac{rF_x - T_b}{J} \tag{6}$$

Friction force of a wheel is given by:

$$F_x = \left(\sigma_0 z + \sigma_1 \frac{dz}{dt} + \sigma_2 v \right) F_z \tag{7}$$

Longitudinal wheel slip is given by:

$$\lambda = \frac{v - \omega r}{v} \tag{8}$$

2.2. Hydraulic brake dynamics

Hydraulic pressure of the wheel cylinder impacts on the brake torque. Solenoid valves regulate the pressure. The braking model with solenoid valves can be considered as a 2nd order system function [16].

$$H(s) = \frac{\omega_n^2}{(s^2 + 2\xi\omega_n s + \omega_n^2)} \tag{9}$$

$p(t)$ - wheel cylinder pressure and braking torque:

$$T_b = K_b p(t) \tag{10}$$

2.3. Combined system dynamics

Let $x_1 = \frac{v}{r}$, $x_2 = \omega$ is considered as two state variables and the output variable is $y = \lambda$. From Eqs. (1) to (5):

$$\frac{dx_1}{dt} = -\left(\frac{F_z}{mr}\right)\left(\sigma_0 z + \sigma_1 \frac{dz}{dt} + \sigma_2 v\right) \tag{11}$$

$$\frac{dx_2}{dt} = -\left(\frac{rF_z}{J}\right)\left(\sigma_0 z + \sigma_1 \frac{dz}{dt} + \sigma_2 v\right) - \left(\frac{T_b}{J}\right) \tag{12}$$

$$\text{and } y = \lambda \tag{13}$$

Differentiating Eq. (13) results:

$$\begin{aligned} \frac{dy}{dt} &= \frac{d\lambda}{dt} \\ &= \frac{d}{dt} [1 - (\omega r / v)] \\ &= \frac{d}{dt} [1 - (x_2 / x_1)] \\ &= \frac{\frac{d(x_1 - x_2)}{dt}}{x_1} \end{aligned} \tag{14}$$

Substituting values of x_1 , x_2 from Eqs. (11), (12) and (14), results:

$$\begin{aligned} \frac{dy}{dt} &= \frac{1}{x_1} \left[-\left(\frac{F_z}{mr}\right)\left(\sigma_0 z + \sigma_1 \frac{dz}{dt} + \sigma_2 v\right) (1 - \lambda) - \left(\frac{rF_z}{J}\right)\left(\sigma_0 z + \sigma_1 \frac{dz}{dt} + \sigma_2 v\right) \right. \\ &\quad \left. + \left(\frac{T_b}{J}\right) \right] \\ &= \frac{1}{x_1} \left[\left(\sigma_0 z + \sigma_1 \frac{dz}{dt} + \sigma_2 v\right) \left(-\frac{F_z}{mr} (1 - \lambda) - \frac{rF_z}{J}\right) + \left(\frac{T_b}{J}\right) \right] \end{aligned} \tag{15}$$

3. Wheel Slip Control using Bang-Bang Controller

Bang-Bang controller is basically the on-off controller. It is standard signum function used to maintain the wheel slip within the desired range. ABS system continuously monitors the wheel slip value and compares it with desired slip value,

usually 0.2 and makes an error to be zero. This action occurs whenever the Brake torque value T_B occurs a maximum value [17, 18]. The contents of the control block are elaborated in Sections 5 and 6. Its place within the simulation is after the sensor block. The model is a closed-loop control system, in which, the controller uses sensor data to determine a reference signal for the actuator [19].

4. Wheel Slip Control using Sliding Mode Controller

The control objective is to drive the wheel slip ratio λ to the desired constant value λ_d , which is the reference input to the SMC. The controller is used to track the reference wheel slip, hence, the sliding surface can be defined as:

$$s = \left(\frac{d}{dt} + \gamma\right)^{r-1} (\lambda - \lambda_d) \quad (16)$$

Output system relative order r follows unity. Hence,

$$s = \lambda - \lambda_d \quad (17)$$

When the state (λ, λ) reaches the switching subspace defined by $s = 0$, it causes sliding motion to occur. Equivalent control keeps the system state trajectory on the switching subspace.

Sliding surface dynamics is represented by:

$$\dot{s} = 0 \quad (18)$$

Differentiating Eq. (17) on both sides, we have:

$$\dot{s} = \dot{\lambda}, \lambda_d \text{ being a constant value.}$$

Combining Eqs. (15), (18) we have,

$$\frac{1}{x_1} \left[\left(\sigma_0 z + \sigma_1 \frac{dz}{dt} + \sigma_2 v \right) \left(-\frac{F_z}{mr} (1 - \lambda) - \frac{rF_z}{J} \right) + \left(\frac{T_b}{J} \right) \right] = 0$$

Hence, the equivalent control is given by:

$$T_b = u_{eq}(t) = Jx_1 \left[\left(\frac{\sigma_0 z + \sigma_1 \frac{dz}{dt} + \sigma_2 v}{x_1} \right) \left(\frac{F_z}{mr} (1 - \lambda) + \frac{rF_z}{J} \right) \right] \quad (19)$$

Additional control term called hitting control is added to equivalent control when system state trajectory is not on the switching subspace. That is:

$$u(t) = u_{eq}(t) + u_s(t) \quad (20)$$

$$s(t)\dot{s}(t) < 0 \text{ reaching condition is obeyed} \quad (21)$$

System state trajectory is always directed towards the sliding surface by satisfying the reaching condition (4.6). Hitting control input used is given by:

$$u_s(t) = - \left(Jx_1 \rho \frac{s(t)}{|s(t)| + \delta} \right) \quad (22)$$

Chattering problem is reduced by selecting the term boundary layer thickness δ and designer parameter, ρ . Reaching condition is evaluated by considering,

$$s(t)\dot{s}(t) = s(t) \left[\frac{1}{x_1} \left[\left(\sigma_0 z + \sigma_1 \frac{dz}{dt} + \sigma_2 v \right) \left(-\alpha(1 - \lambda) - \beta \right) + \frac{T_b}{J} \right] \right] \text{ where}$$

$$\begin{aligned} \alpha &= \frac{F_z}{mr} \text{ and } \beta = \frac{rF_z}{J} \text{ are two constants.} \\ &= s(t) \left[\frac{1}{x_1} \left[\left(\sigma_0 z + \sigma_1 \frac{dz}{dt} + \sigma_2 v \right) (-\alpha(1-\lambda) - \beta) + \frac{u(t)}{J} \right] \right], \text{ where } T_b = u(t) \\ &= s(t) \left[\frac{1}{x_1} \left[\left(\sigma_0 z + \sigma_1 \frac{dz}{dt} + \sigma_2 v \right) (-\alpha(1-\lambda) - \beta) \right. \right. \\ &\quad \left. \left. + \frac{1}{x_1} \left[\left(\sigma_0 z + \sigma_1 \frac{dz}{dt} + \sigma_2 v \right) (\alpha(1-\lambda) + \beta) - \rho \frac{s(t)}{|s(t)| + \delta} \right] \right] \right] \\ &= s(t) \left[\rho \frac{s(t)}{|s(t)| + \delta} \right] \end{aligned}$$

Hence, the sliding mode condition is satisfied for $\rho > 0$.

Hence, for $\rho > 0$, control law $u(t) = u_{eq}(t) + u_s(t)$ drives the system state trajectory on to the sliding surface and leftovers on it later [20]. The simulation parameters used in the simulation is tabulated below shown in Tables 1 and 2.

Table 1. Parameters used in simulation.

Parameter	Value
g	9.8 m/s ²
J	1.7 kg m ²
ε	354
v	70 m/s
r	0.326 m
ω_h	7.07 s ⁻¹
m	375 kg
ρ	500
Kb	100
δ	1 mm

Note: Boundary layer thickness $\delta = 0.005$ for dry asphalt and $\delta = 0.013$ for icy road. LuGre Friction parameters are given below:

Table 2. LuGre friction parameters.

Parameter	Value
σ_0	10 ⁵ N/m
σ_1	$\sqrt{10^5}$ Ns/m
σ_2	0.4 Ns/m
μ_s	1.5 N
μ_c	1 N
v_s	0.001 m/s

5. Burckhardt Friction Model

Burckhardt friction model, which is essentially a static friction model, is implemented in ABS mathematical model, which employs a quarter car vehicle mode and brake actuator model, the regulation of wheel slip at the desired value is achieved by using SMC algorithm.

To simulate ABS controlling action tire friction model introduced by Burckhardt has been utilized as in Table 3. Li et al. [21] and Kerst et al. [22]

reported that it gives the friction coefficient μ is a function of wheel slip and vehicle speed.

$$\mu(\lambda, v) = [c_1(1 - e^{-c_2\lambda}) - c_3\lambda]e^{-c_4\lambda v} \quad (23)$$

Table 3. Friction model parameters.

Road surface	c_1	c_2	c_3
Dry asphalt	1.28	23.99	0.52
Wet asphalt	0.85	33.82	0.34
Dry concrete	0.19	94.12	0.06
Snow	0.19	94.12	0.06
Ice	0.05	306.39	0

5.1. Integrated system dynamics

Let $x_1 = \frac{v}{r}$, $x_2 = \omega$ is considered as two state variables and the output variable is $y = \lambda$.

From Eqs. (23), (5) to (7),

$$\frac{dx_1}{dt} = -\frac{F_z}{mr} [(C_1(1 - e^{-c_2\lambda}) - c_3\lambda)e^{-c_4\lambda v}] \quad (24)$$

$mr = \frac{J}{r}$ and subtracting the ratio $\frac{T_b}{J}$

$$\frac{dx_1}{dt} = \left(\frac{rF_z}{J}\right) [(C_1(1 - e^{-c_2\lambda}) - c_3\lambda)e^{-c_4\lambda v}] \cdot \frac{T_b}{J} \quad \text{and} \quad (25)$$

$$y = \lambda \quad (26)$$

Now, differentiating the output Eq. (26), we have,

$$\begin{aligned} \frac{dy}{dt} &= \frac{d\lambda}{dt} \\ &= \frac{d}{dt} [1 - (\omega r/v)] \\ &= \frac{d}{dt} [1 - (x_2/x_1)] \\ &= \frac{\frac{dx_1}{dt}(1-\lambda) - x_2}{x_1} \end{aligned} \quad (27)$$

Now, substituting the values of \dot{x}_1 , \dot{x}_2 from Eqs. (24), (25) and (27), results:

$$\frac{dy}{dt} = \frac{1}{x_1} \{ [C_1(1 - e^{-c_2\lambda}) - c_3\lambda]e^{-c_4\lambda v} \} \left(-\frac{F_z}{mr} (1 - \lambda) - \frac{rF_z}{J} \right) + \frac{T_b}{J} \quad (28)$$

6. Proposed SMC Controller

The goal of an ABS controller is to discharge the wheel speed while vehicle panic braking. The ideal slip is somewhere in the range of 0.15 and 0.25, contingent upon the type of road surface. The associations among wheel and road surface can be demonstrated as the following articulation.

$$\dot{\omega}_i = -(K_i u_i + \tau_{xi} + \tau_{ri}) \quad (29)$$

where $K_i = \frac{AR_b}{I_{wi}}$, $\tau_{xi} = \frac{F_{xi}R_w}{I_{wi}}$, $\tau_{ri} = \frac{F_{ri}f_{ri}}{I_{wi}}$ and P_{wi} is defined as control input, u_i , torque from a control engine T_{eng} is zero.

Proposed sliding mode controller is defined as:

$$s = -\left(\frac{d}{dt} + \lambda\right)^{n-1} \int_0^t \lambda_x dr \tag{30}$$

where λ is a strictly positive constant, $\lambda_r = \lambda_{di} - \lambda_i$ is desired slip (typically its value is 0.2) and $n = 2$. Based on the condition $S = 0$ of nonstop control, the following \hat{u}_i is given by:

$$\hat{u}_i = -\frac{1}{v_x K_i} \left[(\hat{t}_{xi} + \hat{t}_{yi})v_x + \omega_i v_x - \frac{v_x^2 \lambda}{R_w} (\lambda_{si} - \lambda_{di}) \right] \tag{31}$$

Equation (31) is valid by assuming that estimation zero error of braking torque. Discrete function \bar{u}_i defined as Eq. (32) is added to Eq. (31), since the assumption is not correct.

$$\bar{u}_i = \frac{\hat{t}_{xi} + \hat{t}_{ri} + \eta}{K_i} \text{Sgn}(S) \tag{32}$$

η is strictly > 0 .

From the Eqs. (31) and (33), the control input u_i can be obtained as given below:

$$u_i = \hat{u}_i + \bar{u}_i = -\frac{1}{v_x K_i} \left[(\hat{t}_{xi} + \hat{t}_{yi})v_x + \omega_i v_x - \frac{v_x^2 \lambda}{R_w} (\lambda_{si} - \lambda_{di}) \right] + \frac{\hat{t}_{xi} + \hat{t}_{ri} + \eta}{K_i} \text{Sgn}(S) \tag{33}$$

By changing $\text{sgn}(S)$ to $\text{sat}(S)$, the chattering problem caused by discontinuity of the $\text{sgn}(S)$ can be adjusted.

7. Results and Discussion

Results and discussions are carried out in two sections; in Section 7.1 describe the simulation of longitudinal dynamics behaviour of a vehicle in the absence and presence of the braking controller. Section 7.2 mainly focus on the performance comparison of various controllers.

7.1. Simulation of longitudinal dynamics

7.1.1. Scenario 1. In absence of braking controller

Figure 2 depicts the behaviour of the angular velocity of rear-wheel measured in rad/seconds, in absence of braking controller. The angular velocity of the wheel is increased linearly as the acceleration increases. The angular speed of the wheel maintains the constant rate as the acceleration of the vehicle to be maintained at a constant value. At approximately the time $t = 175$ seconds, the brake torque is applied as a result the wheel angular speed is decreased slowly and reaches to zero as the brake torque is maintained.

Figure 3 depicts the behaviour of vehicle velocity of rear-wheel measured in m/s, in absence of braking controller. The vehicle velocity of the wheel is increased linearly as the acceleration increases. Vehicle velocity maintains the constant rate as the acceleration of the vehicle to be maintained at a constant value. At approximately the time $t = 185$ seconds, the brake torque is applied as a result the

vehicle velocity is decreasing slowly and reaches to zero as the brake torque is maintained. From Figs. 2 and 3, it is observed that the angular velocity of the wheel and the vehicle velocity both are linearly related to each other. As vehicle velocity changes linearly with the angular speed of the vehicle vice versa.

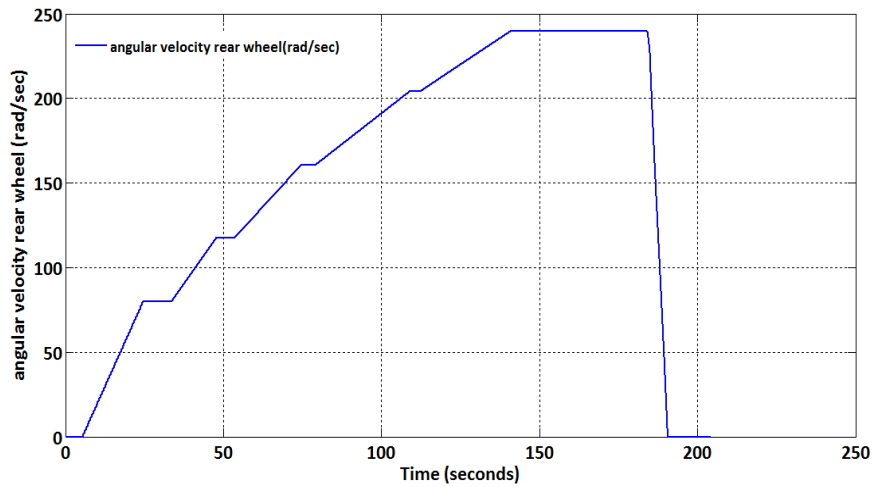


Fig. 2. Angular velocity of rear-wheel (rad/s).

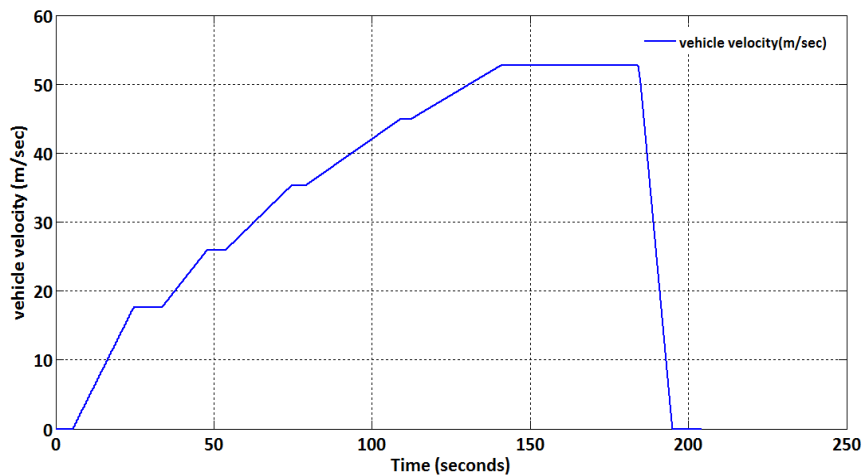


Fig. 3. Vehicle velocity (m/s).

Figure 4 depicts the behaviour of rear-wheel slip (λ), in absence of braking controller. The minimum value of λ is zero that is when the vehicle velocity and angular velocity of the wheel both are equal. The maximum value of λ is 1.

Figure 5 depicts the behaviour of vehicle rear brake torque measured in newton meters. At $t = 175$ seconds the brake torque is applied with a value of around 570 N-m, as a result, the wheel angular velocity and vehicle speed decreases.

The braking scenario in the absence of a controller is depicted in Fig. 6. Here it has been observed that initially the angular wheel velocity and vehicle velocity both are varied linearly. During this scenario, the wheel slip maintains a zero value, results in vehicle not to slip. The moment brake torque is applied at $t = 175$ seconds, results wheel angular velocity suddenly come down to zero, which leads to the wheel will get suddenly locks up but still, vehicle maintains some velocity due to the moment of inertia. As a result, vehicle velocity is slowly come down to zero after the wheel locks up. This shows that whenever braking occurs the wheel angular velocity is not synchronous with the vehicle velocity. This leads vehicle to spin. In order to achieve a vehicle not to spin, it is necessary to maintain the wheel slip value within the desired range. In order to achieve this, it is necessary to have a controlling action within the braking module.

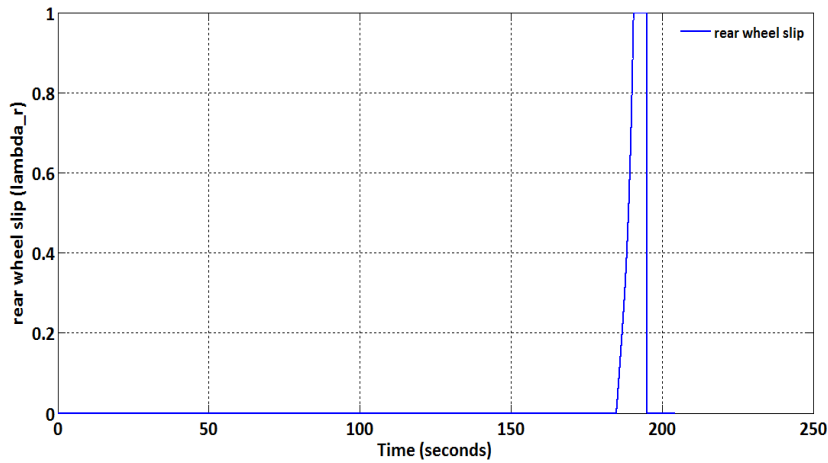


Fig. 4. Rear-wheel slip.

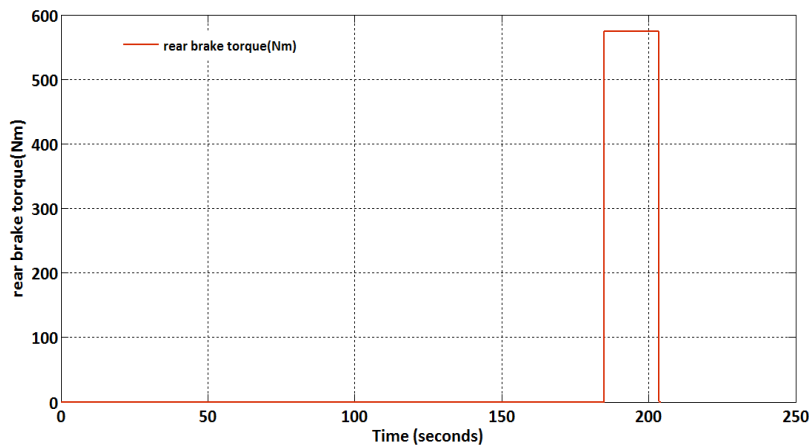


Fig. 5. Rear brake torque (N-m).

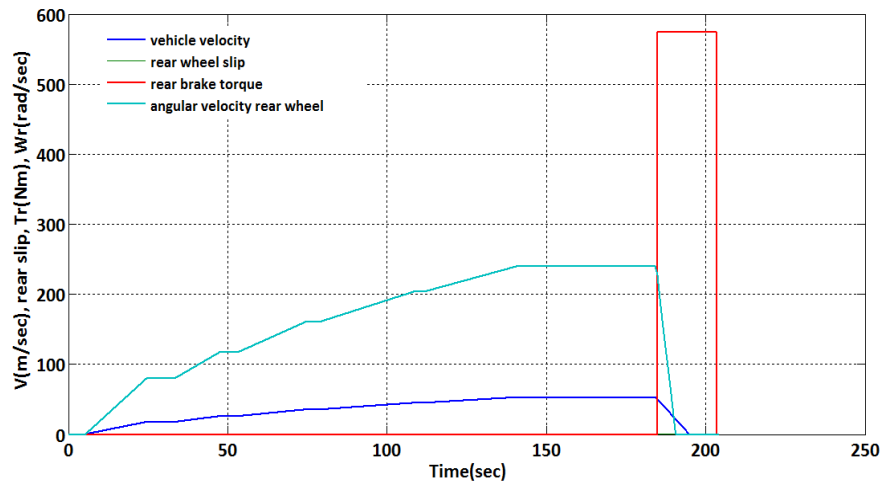


Fig. 6. Braking scenario in absence of controller.

7.1.2. Scenario 2. In presence of braking controller

Figure 7 depicts the behaviour of the angular velocity of rear-wheel measured in rad/seconds, in presence of a braking controller. The angular velocity of the wheel is increased linearly as the acceleration increases. The angular speed of the wheel maintains the constant rate as the acceleration of the vehicle to be maintained at a constant value. At approximately the time $t = 165$ seconds, the brake torque is applied as a result the wheel angular speed is decreased slowly and reaches to zero as the brake torque is maintained.

Figure 8 depicts the behaviour of vehicle velocity of rear-wheel measured in meter/seconds, in presence of a braking controller. The vehicle velocity of the wheel is increased linearly as the acceleration increases. Vehicle velocity maintains the constant rate as the acceleration of the vehicle to be maintained at a constant value. At approximately the time $t = 165$ seconds, the brake torque is applied as a result the vehicle velocity is decreasing slowly and reaches to zero as the brake torque is maintained.

From Figs. 7 and 8, it is observed that the angular velocity of the wheel and the vehicle velocity both are linearly related to each other. As vehicle velocity changes linearly with the angular speed of the vehicle vice versa.

Figure 9 depicts the behaviour of rear-wheel slip (λ), in the presence of a braking controller. The minimum value of λ is zero that is when the vehicle velocity and angular velocity of the wheel both are equal. The maximum value of λ is 1. This occurs when brake torque is applied suddenly the wheel locks results the angular velocity of the wheel will come down to zero but due to the inertia still vehicle maintains some vehicle velocity, therefore, the wheel slip reaches to its maximum value that is one.

This scenario can be seen from the figure that is at $t = 165$ seconds the brake torque is applied as a result the wheel slip is modulation occurs that is within 165 to 175 seconds the brake pressure modulation takes place as a result wheel will never suddenly locks because the slip value is maintained within the desired range.

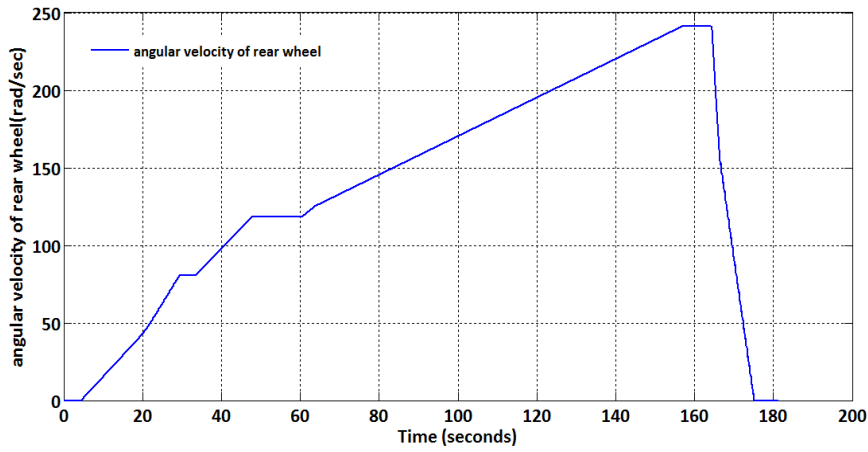


Fig. 7. Rear-wheel angular velocity (rad/s).

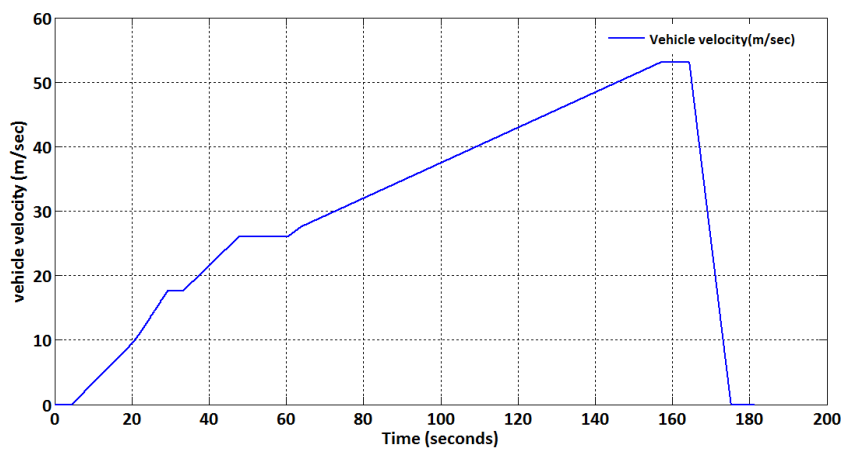


Fig. 8. Vehicle velocity (m/s).



Fig. 9. Rear-wheel slip.

Figure 10 depicts the behaviour of vehicle rear brake torque measured in Newton meters. At $t = 165$ seconds the brake torque is applied with a value of around 570 N-m, as a result, the brake pressure modulation takes place and slip value is maintained within the desired range. Therefore, wheel angular velocity and vehicle speed synchronized, that is both will become down to zero at the same time.

The braking scenario in presence of controller is depicted in Fig. 11. Here it has been observed that initially the angular wheel velocity and vehicle velocity both are varied linearly. During this scenario, the wheel slip maintains a zero value, results in vehicle not to slip. The moment brake torque is applied at $t = 165$ seconds, results brake pressure modulation takes place, therefore, wheel angular velocity and vehicle velocity will come down to zero at the same time, in which, leads wheel will never be locked up suddenly but vehicle velocity is get synchronized with wheel angular velocity. This leads vehicle will never undergo spinning condition and it will stay remain in a stable zone. In order to achieve a vehicle not to spin, it is necessary to maintain the wheel slip value within the desired range. In order to achieve this, it is necessary to have an SMC controlling activities within the braking module.

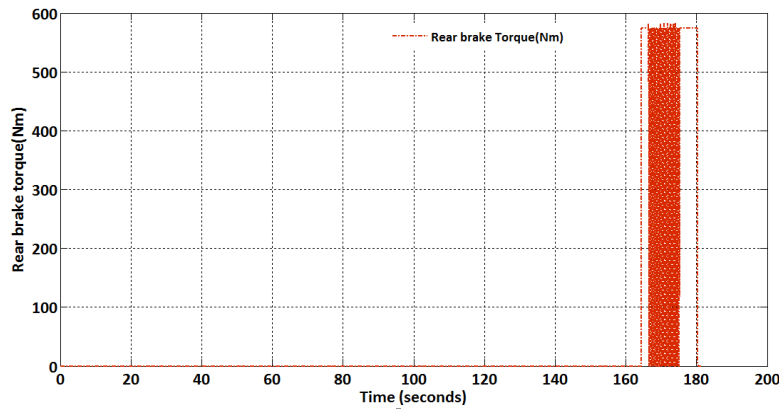


Fig. 10. Rear brake torque (N-m).

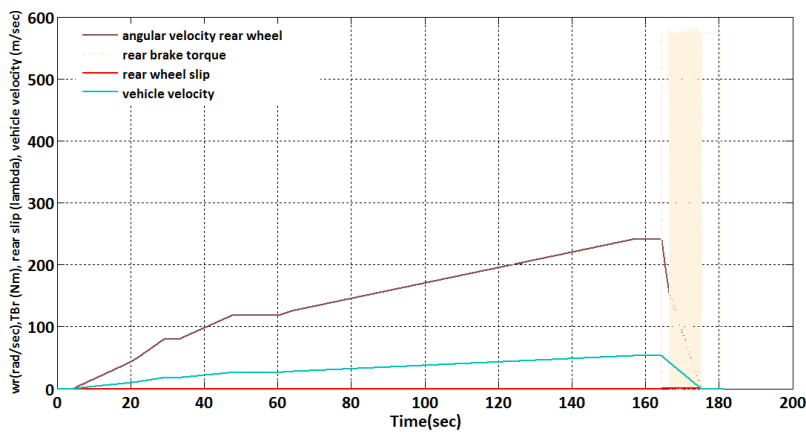


Fig. 11. Braking scenario in presence of SMC.

7.2. Performance comparison

Figure 12 depicts the behaviour of wheel slip under braking scenario. In absence of braking controller, it has been observed from the figure the moment brake torque applied, wheel slip will reach to its maximum value that is one. This leads wheel will get suddenly locks up. In order to avoid wheel lock, various controller techniques are introduced. Depending on the control strategies of the controller the wheel slip value is maintained within the threshold value, normally the desired value of the slip is 0.2. However, from the simulation results, the proposed SMC technique can achieve the threshold value below the 0.2. That is the slip modulation occurs in the range between 0.1 and below the 0.2. The least threshold slip can be achieved with the proposed SMC controller compared to the existing control techniques.

Figure 13 depicts the behaviour of wheel velocity under braking scenario. In absence of braking controller, it has been observed from the figure the moment brake torque applied, wheel locks up suddenly as a result wheel velocity come downs to zero. In presence of a braking controller, wheel velocity will be always synchronous with the vehicle velocity. The proposed SMC controller gives the optimal wheel velocity then compared to the existing controller. From the simulation result, the wheel velocity modulation can be observed.

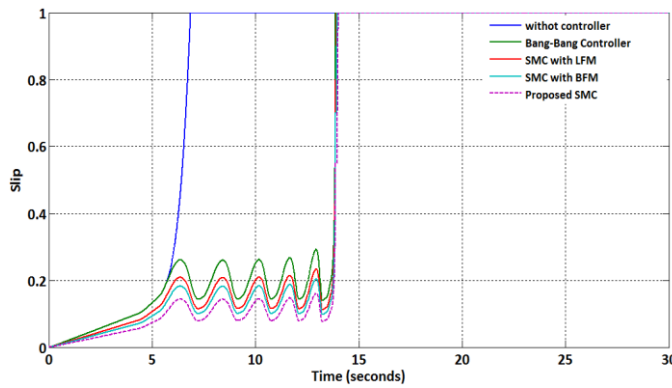


Fig. 12. Wheel slip.

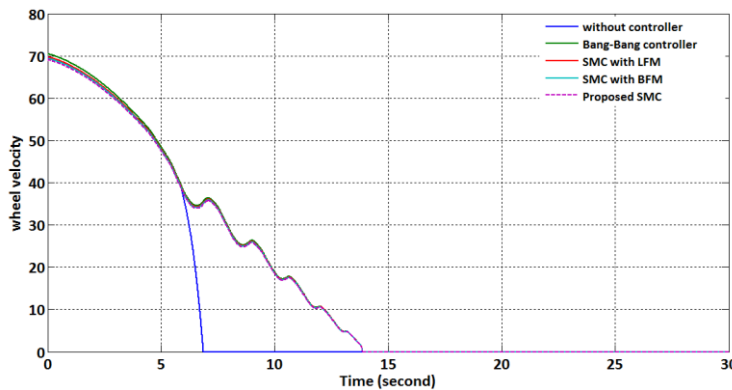


Fig. 13. Wheel velocity (m/s).

Figure 14 depicts the behaviour of vehicle velocity under braking scenario. In absence of braking controller, it has been observed from the figure the moment brake torque applied, wheel locks up suddenly as a result vehicle velocity come downs to zero but it is not in synchronous with the wheel angular velocity and also it takes little more time to reach zero. In presence of a braking controller, vehicle velocity will be always synchronous with the wheel angular velocity. The proposed SMC controller gives the optimal vehicle velocity then compared to the existing controller. From the figure vehicle, velocity is reaching to zero faster than the existing methods.

Figure 15 depicts the stopping distance measured in meters under various scenarios. From the simulation results, it is very clear that in the absence of the braking controller under the braking scenario, the vehicle stopping distance takes almost 100 meters. In the presence of a braking controller that is bang-bang controller, it achieves the braking distance of 70 meters, correspondingly the SMC with LFM method gives 58 meters and SMC with BFM control method gives the 50 meters. The proposed SMC controller achieves stopping distance of 40 meters, which is the least stopping distance compared to all other techniques.

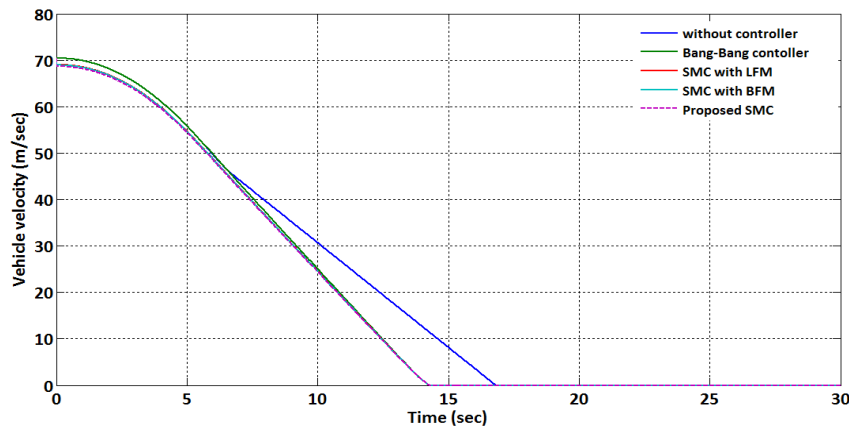


Fig. 14. Vehicle velocity (m/s).

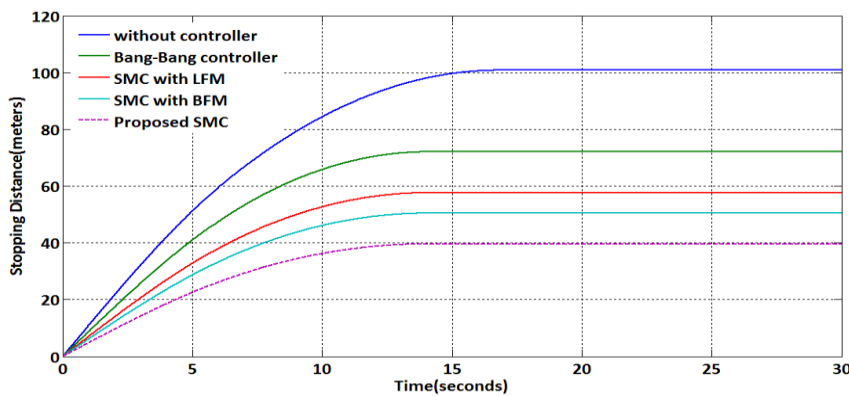


Fig. 15. Stopping distance (m).

8. Conclusion

This paper presents the modelling of a novel ABS algorithm based on wheel force and slip data. The designed ABS algorithm results in the encirclement of the friction coefficient peak. It is based on two phases: one ensures a decreasing wheel slip, other guarantees an increasing wheel slip. The control algorithm depends on references that describe the optimal friction coefficient and wheel slip. The maximum friction coefficient and its corresponding wheel slip value are considered the optima value that is 0.12, however, the desired value is 0.2 and the range varies from 0.12 to 0.22. Triggering occurs based on the deviation of the measurement values with respect to these optima. The output of the controller, a brake torque reference, is based on this information and prevents the wheels from locking. The simulation results are evident to conclude that, the proposed SMC controller gives the better performance in terms of brake pressure modulation, maintaining the wheel slip value within the threshold range, in terms of the vehicle stopping time and vehicle stopping distance.

Nomenclatures

c_1	Is the maximum value friction curve
c_2	Friction curve shape
c_3	Friction curve difference between the maximum value and the value at $\lambda = 1$
c_4	Wetness characteristics value and is in range 0.02 to 0.04 s/m
F_x	Tractive force, N
F_z	Normal/vertical load, N
g	Acceleration due to gravity, m/s ²
J	Moment of inertia of wheel, kg.m ²
K_b	Torgue gain
m	Quarter vehicle mass, kg
r	Rolling radius of wheel, m
T_b	Braking torque, N.m
v	Vehicle absolute velocity, m/s
v_s	Stribeck velocity, $-v_s, < v < v_s$, m/s

Greek Symbols

μ_c	Normalized kinetic friction force or Coulumb friction level
μ_s	Normalized static friction force
ξ	Damped ratio of braking system
σ_o	Aggregate bristle stiffness
σ_1	Damping coefficient
σ_2	Account for viscous friction
ω	Wheel angular speed
ω_n	Undamped natural frequency

References

1. Hagenzieker, M.P.; Commandeur, J.J.F.; and Bijleveld, F.D. (2014). The history of road safety research: A quantitative approach. *Transportation Research Part F: Traffic Psychology and Behavior*, 25, Part B, 150-162.

2. Hulten, J. (2006). Active safety introduction. *Volvo Car Corporation Presentation at CTH*.
3. Khan, Y.; Kulkarni, P.; and Youcef-Toumi, K. (2014). Modeling, experimentation and simulation of a brake apply system. *Journal of Dynamic Systems, Measurement, and Control*, 116(1), 111-122.
4. Raza, H.; Xu, Z.; Yang, B.; and lounnau, P.A. (2017). Modeling and control design for computer-controlled brake system. *IEEE Transactions on Control System Technology*, 5(3), 279-296.
5. Gowda, D.V.; Kishore, D.V.; Shivashankar; Ramachandra, A.C.; and Pandurangappa, C. (2016). Optimization of motorcycle pitch with nonlinear control. *Proceedings of the 1st IEEE International Conference on Recent Trends in Electronics, Information and Communication Technology (RTEICT)*. Bangalore, India, 1656-1660.
6. Gerdes, J.C.; and Herdrick, J.K. (2015). Brake system modeling for simulation and control. *Journal of Dynamic Systems, Measurement, and Control*, 121(3), 496-503.
7. Johnson, C.T.; and Lorenz, R.D. (2016). Experimental identification of friction and its compensation in precise, position controlled mechanisms. *IEEE Transactions on Industry Applications*, 28(6), 1392-1398.
8. Pandurangappa, C.; Gowda, D.V.; Kishore, D.V.; and Ramachandra, A.C. (2016). Two wheeler vehicle model development for driving simulator application. *GIT Journal of Engineering and Technology*, 9(1), 47-51.
9. Sohl, G.A.; and Bobrow, J.E. (2016). Experiments and simulations on the nonlinear control of a hydraulic servosystem. *IEEE Transactions on Control Systems Technology*, 7(2), 238-247.
10. Srinivasa, R.; Guntur, R.R.; and Wong, J.Y. (2016). Evaluation of the anti-lock brake systems using laboratory simulation techniques. *Vehicle Design*, 1(5), 467-484.
11. Gowda, D.V.; and Chakrasali, S. (2014). Comparative analysis of passive and semi-active suspension system for quarter car model using PID controller. *Proceedings of the International Conference on Recent Trends in Signal Processing, Image Processing and VLSI (ICrSIV)*. Karnataka, India, 510-517.
12. Ackermann, J.; and Sieneel, W. (2015). Robust yaw damping of cars with front and rear wheel steering. *IEEE Transactions on Control Systems Technology*, 1(1), 15-20.
13. Davison, E. and Ferguson, I. (2016). The design of controllers for multivariable robust servomechanism problem using parameter optimization methods. *IEEE Transactions on Automatic Control*, 26(1), 93-110.
14. Gowda, D.V.; and Ramachandra, A.C. (2017). Slip ratio control of anti-lock braking system with bang-bang controller. *International Journal of Computer Techniques*, 4(1), 97-104.
15. Usal, C.; and Kachroo, P. (2017). Sliding mode measurement feedback control for antilock braking systems. *IEEE Transaction Control Systems Technology*, 7(2), 271-281.
16. Utkin, V.I. (2016). Sliding mode control design principles and applications to electric drives. *IEEE Transactions Industrial Electronics*, 40(1), 23-36.

17. Schinkel, M.; and Hunt, K. (2012). Anti-lock braking control using a sliding mode like approach. *Proceedings of the American Control Conference*. Anchorage, Alaska, 2386-2391.
18. Lee, H.; and Tomizuka, M. (2016). Adaptive vehicle traction force control for intelligent vehicle highway systems (IVHSs). *IEEE Transactions on Industrial Electronics*, 50(1), 37-47.
19. Gowda, D.V.; and Ramachandra, A.C. (2018). Importance of non-linear controller in implementing anti-lock braking system-a technical review. *International Journal of Advanced Research in Computer Science*, 9(2), 193-199.
20. Lee, H.; and Utkin, V.I. (2013). Chattering suppression method in sliding mode control system. *Annual Reviews in Control*, 31(2), 179-188.
21. Li, L.; Wang, F.-Y.; and Zhou, Q. (2015). Integrated longitudinal and lateral tire/road friction modeling and monitoring for vehicle motion control. *IEEE Transactions on Intelligent Transportation Systems*, 7(1), 1-19.
22. Kerst, S.; Shyrokau, B.; and Holweg, E. (2016). Reconstruction of wheel forces using an intelligent bearing. *SAE International Journal of Passenger Cars-Electronic and Electrical Systems*, 9(1), 196-203.